

Two-body scattering in a trap and a special periodic phenomenon sensitive to the interaction

Y. Z. He and C. G. Bao*

*State Key Laboratory of Optoelectronic Materials and Technologies,
Sun Yat-Sen University, Guangzhou, 510275, P.R. China*

Two-body scattering of neutral particles in a trap is studied theoretically. The control of the initial state is realized by using optical traps. The collisions inside the trap occur repeatedly; thereby the effect of interaction can be accumulated. Two periodic phenomena with a shorter and a much longer period, respectively, are found. The latter is sensitive to the interaction. Instead of measuring the differential cross section as usually does, the measurement of the longer period and the details of the periodic behavior might be a valid source of information on weak interactions among neutral particles.

PACS numbers: 34.10.+x, 34.90.+q, 34.50.Cx, 37.10.-x

The determination of interactions among microscopic particles is an important topic in physics. Historically, the measurement of the cross sections of 2-body scattering provides an important source of information. For neutral atoms and molecules the determination is more difficult because the interaction is in general weak and the initial momentum of the incident particle is difficult to be precisely controlled. However, if the scattering occurs in a trap, new phenomena previously unknown might emerge. Due to the recent progress in the techniques of trapping atoms (molecules) by using optical traps [1–3], trapped scattering might be eventually experimentally realized. In a previous paper a model was proposed to study the trapped 2-body scattering theoretically [4]. Instead of a single collision, numerous repeated collisions have been found. Thereby the effect of interaction can be accumulated and enlarged, and might be eventually detected. This favors the determination of very weak interaction. The emphasis of that paper is placed on the study of the spin-flip phenomenon and the determination of the parameter g_0 (the strength of the channel with total spin zero) of the ^{52}Cr atoms. This paper is also dedicated to trapped scatterings; however the emphasis is placed on the study of a specific periodicity emerging from the repeated collisions. It turns out that the associated period is sensitive to the interaction. Therefore, in addition to the measurement of cross sections, the observation of the special periodic phenomenon might be also a valid way for the determination of interaction. The model, related theoretical derivation, and numerical results are given below.

We propose a device containing two deep optical traps initially. One is close to the origin, while the other one is far away. Each trap provides a harmonic potential. Thus the total potential was $U_p(\mathbf{r}) = \frac{1}{2}\mathcal{M}\omega_p^2(|\mathbf{r} - \mathbf{a}|^2 + |\mathbf{r} - \mathbf{b}|^2)$, where \mathbf{a} and \mathbf{b} are two given vector (norms $a \gg b$), and \mathcal{M} is the mass of the particle involved.

Each trap contains a particle in the lowest harmonic oscillator (h.o.) state. The two particles are assumed to be identical bosons (the generalization to fermions is straight forward), the interaction is assumed to be spin-independent, and ω_p is large enough so that the particles are well localized initially and the overlap of their wave functions is negligible. Suddenly the two deep traps are cancelled. Instead, a broader new trap located at the origin $U_{evol}(r) = \frac{1}{2}\mathcal{M}\omega^2 r^2$ is created, $\omega < \omega_p$. Since the initial state is not an eigenstate of the new Hamiltonian, the system begins to evolve. The evolution is affected not only by $U_{evol}(r)$ but also by the interaction $V(|\mathbf{r}_i - \mathbf{r}_j|)$. In what follows the details of the evolution is studied, two-body collisions occurring repeatedly are found, and the effect of interaction is demonstrated.

Let $\hbar\omega$ and $\sqrt{\hbar/\mathcal{M}\omega}$ be used as units of energy and length. The normalized initial state is

$$\Psi_I = \frac{1}{\sqrt{2}}(1+P_{1,2})\left(\frac{\eta}{\pi}\right)^{\frac{6}{4}} \exp\left[-\frac{\eta}{2}(|\mathbf{r}_1 - \mathbf{a}|^2 + |\mathbf{r}_2 - \mathbf{b}|^2)\right] \quad (1)$$

where $P_{1,2}$ implies an interchange of 1 and 2, and $\eta = \omega_p/\omega$. We consider the case that \mathbf{a} is lying along the X -axis, while \mathbf{b} along the negative Z -axis. When $\mathbf{R} = (\mathbf{r}_1 + \mathbf{r}_2)/2$ and $\mathbf{r} = \mathbf{r}_2 - \mathbf{r}_1$ for the c.m. and relative motions, respectively, are introduced, and the h.o. states of the new trap are selected as base functions, the initial state can be expanded as

$$\Psi_I = \sum_{N L n l J M} B_{N L n l}^{J M} [\varphi_{N L}^{(2)}(\mathbf{R}) \varphi_{n l}^{(1/2)}(\mathbf{r})]_{J M} \quad (2)$$

where $\varphi_{n l}^{(\mu)}(\mathbf{r})$ is a normalized eigenstates of the Hamiltonian $-\frac{1}{2\mu}\nabla_{\mathbf{r}}^2 + \frac{1}{2}\mu r^2$ with the eigenenergy $2n + l + 3/2$. L and l are coupled to the total orbital angular momentum

*Corresponding author: stsbcg@mail.sysu.edu.cn

J and M .

$$\begin{aligned}
B_{NLnl}^{JM} &= \sqrt{2} \left(\frac{\eta}{\pi}\right)^{\frac{3}{2}} \sum_m C_{L,M-m,l,m}^{J,M} \\
&\times \left\{ \int d\mathbf{R} \varphi_{N,L,M-m}^{(2)}(\mathbf{R}) \right. \\
&\times \left. e^{-\frac{\eta}{2}[2R^2+a^2-2R(a\sin\theta_R\cos\phi_R-b\cos\theta_R)]} \right\} \\
&\times \left\{ \int d\mathbf{r} \varphi_{nlm}^{(1/2)}(\mathbf{r}) \right. \\
&\times \left. e^{-\frac{\eta}{2}[\frac{1}{2}r^2+b^2+r(a\sin\theta_r\cos\phi_r+b\cos\theta_r)]} \right\} \quad (3)
\end{aligned}$$

where the Clebsch-Gordan coefficients are introduced, θ_R and ϕ_R are the spherical polar coordinates, and so on, l must be even for boson systems.

The new Hamiltonian in terms of \mathbf{R} and \mathbf{r} governing the evolution is

$$\begin{cases} H_{evol} = H_R + H_r \\ H_R = -\frac{1}{4}\nabla_{\mathbf{R}}^2 + R^2 \\ H_r = -\nabla_{\mathbf{r}}^2 + \frac{1}{4}r^2 + V(r) \end{cases} \quad (4)$$

Using $\varphi_{nl}^{(1/2)}$ as base functions, the eigenstates of H_r can be obtained via a diagonalization and can be expanded as

$$\psi_{l,i}(\mathbf{r}) = \sum_n D_n^{l,i} \varphi_{nl}^{(1/2)}(\mathbf{r}) \quad (5)$$

where i denotes the i -th eigenstate of the l -series in the order of increasing energy. The associated energy is denoted by $E_{l,i}$. Reversely, $\varphi_{nl}^{(1/2)}$ can also be expanded in terms of $\psi_{l,i}$. Then, starting from Ψ_I , the time-dependent solution of H_{evol} is

$$\begin{aligned}
\Psi(\tau) &= e^{-iH_{evol}\tau} \Psi_I \\
&= \sum_{NLnlJM} B_{NLnl}^{JM} \sum_{n'i} D_n^{l,i} D_{n'}^{l,i} e^{-i(2N+L+3/2+E_{l,i})\tau} \\
&\times [\varphi_{NL}^{(2)}(\mathbf{R}) \varphi_{n'l}^{(1/2)}(\mathbf{r})]_{JM} \quad (6)
\end{aligned}$$

where $\tau = \omega t$. In principle, the above solution is exact only if the summation covers infinite terms. However, when the interaction is not strong, qualitatively accurate solutions can be obtained if the number of base functions is large enough. This is shown below.

We define the time-dependent one-body density from $\Psi(\tau)$ as

$$\rho(\mathbf{r}_1, \tau) \equiv \int d\mathbf{r}_2 \Psi^*(\tau) \Psi(\tau) \quad (7)$$

In order to obtain ρ , the Talmi-Moshinsky coefficients relating two sets of coordinates are introduced as

$$\begin{aligned}
&[\varphi_{NL}^{(2)}(\mathbf{R}) \varphi_{n'l}^{(1/2)}(\mathbf{r})]_{JM} \\
&= \sum_{n_1 l_1 n_2 l_2} a_{n_1 l_1 n_2 l_2}^{NLn'l,J} [\varphi_{n_1 l_1}^{(1)}(\mathbf{r}_1) \varphi_{n_2 l_2}^{(1)}(\mathbf{r}_2)]_{JM} \quad (8)
\end{aligned}$$

The analytical form of the coefficients can be found in [5–7]. From Eqs. (6) and (8), making use of the orthonormality of the base functions, the integration in Eq. (7) is

easy to carry out, and it is straight forward to obtain the analytical expression of $\rho(\mathbf{r}_1, \tau)$. Incidentally, since the wave function is symmetrized, the behaviors of the two particles are exactly the same. The observation of only one particle is sufficient.

To obtain numerical results as examples, it is first assumed that $a = 2$, $b = 0$, $\eta = 2$, and the interaction contains a stronger repulsive core and a weaker attractive tail as

$$V(r) = \begin{cases} V_0, & \text{if } r < 0.2 \\ -C_6/r^6, & \text{else} \end{cases} \quad (9)$$

where V_0 and C_6 are positive numbers, and $V_0 \gg C_6$. We define $K = 2(N+n)+L+l$ to control the dimension of the base. Mostly, the base functions with $K \leq K_{\max} = 20$ are adopted in the following calculation.

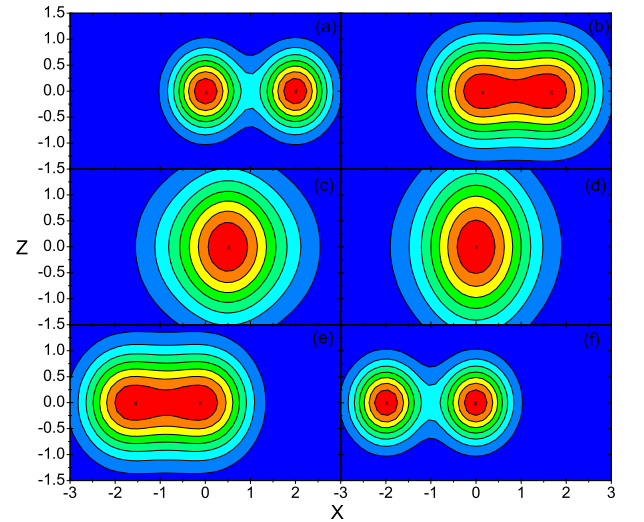


FIG. 1: (Color online) $\rho(\mathbf{r}_1, \tau)$ plotted on the $X - Z$ plane. $\tau = 0, \pi/6, \pi/3, \pi/2, 5\pi/6$ and π , respectively, for (a) to (f). The parameters are $\eta = 2$, $a = 2$, $b = 0$, $V_0 = 10$, $r_0 = 0.2$ and $c_6 = -0.3r_0^6$. The units of energy and length in this paper are $\hbar\omega$ and $\sqrt{\hbar/M\omega}$, where ω has not yet been specified. Every maximum in the panels is marked by a cross. The values associated with the inmost contours of (a) to (f) are 0.224, 0.098, 0.073, 0.063, 0.098 and 0.224. Thus the peaks in (a) and (f) are much higher. Therefore, the particles are better localized when they separate from each other. The values of the outmost contours are from 0.01 to 0.03.

When $V_0 = 10$, $C_6 = -0.3$, and τ is given at a number of values in the early stage of evolution, $\rho(\mathbf{r}_1, \tau)$ plotted on the $X - Z$ plane is shown in Fig. 1. 1a is for the initial case. When the evolution begins, the outside particle moves toward the center and collides with the target particle as shown in 1b and 1c. When $\tau = \pi/2$ both particles are close to the center as in 1d. Afterward a particle begins to leave as in 1e, and will arrive at the opposite end at $\tau = \pi$ as in 1f. Then the process repeats but in reverse direction. When $\tau = 2\pi$ the system recovers its initial status. This is a kind of periodic be-

behavior originating from the harmonic trap. If the interaction is neglected, the recovery would be exact. However, due to the interaction, $\rho(\mathbf{r}_1, \tau)$ is not exactly equal to $\rho(\mathbf{r}_1, \tau + 2\pi)$. With the above parameters, the deviation is very small. Say, when $\mathbf{r}_1 = \mathbf{a}$, we have $\rho(\mathbf{a}, 0) = 0.2553$ and $\rho(\mathbf{a}, 2\pi) = 0.2544$. Obviously, in the period $(0, 2\pi)$ the system undergoes a pair of collisions. When the time goes on, a series of head-on collisions occur repeatedly in the trap. Although the effect of interaction on a round of collision is weak, the effect of many rounds might be accumulated and therefore might become strong. This is shown below.

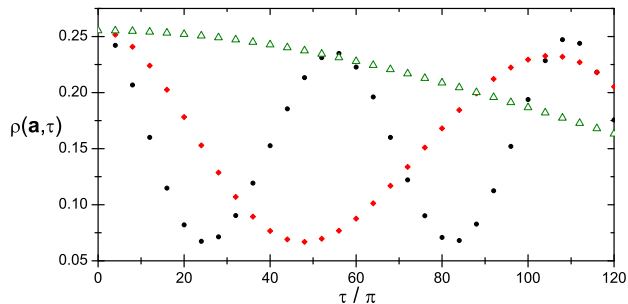


FIG. 2: (Color online) $\rho(\mathbf{a}, \tau)$ plotted against τ , where \mathbf{a} denotes the initial position of the incident particle and τ is given only in discrete values $2k\pi$, where k is an integer from 0 to 60. Three choices of V_0 , namely, 20, 10, and 2 are adopted, and the associated ρ are marked with circles, diamonds, and triangles, respectively (however the values of ρ associated with an odd k have been neglected just for simplicity). The other parameters are the same as in Fig. 1.

In Fig. 2 $\rho(\mathbf{a}, \tau)$ is given at $\tau = 2k\pi$, where k is an integer. It implies that ρ is observed at the initial position of the incident particle repeatedly. If the interaction is removed, all the symbols in the figure would lie along a horizontal line (implying an exact periodicity with a period 2π). However, the interaction causes a deviation. The deviation would become larger if the interaction is stronger (the black circles to be compared with the triangles) and/or if τ is larger. It is found that, when the time goes on, $\rho(\mathbf{a}, 2k\pi)$ against increasing k will first arrive at a minimum, then arrive at the second maximum which is a little lower than the first maximum at $\tau = 0$, then again a minimum, and afterward arrive at the third maximum with a height close to the first maximum. This behavior will repeat again and again. E.g., for $V_0 = 20$ (black circles), the first, second and third maxima appear at $\tau = 0, 54\pi$, and 110π , respectively. Whereas for $V_0 = 10$ (red diamonds), they appear at $0, 104\pi$ and 210π .

On the other hand, making use of the expansion Eq. (6), we calculate the overlap $|\langle \Psi(0) | \Psi(2k\pi) \rangle|$ which varies with k . When k leads to a minimum (maximum) of $\rho(\mathbf{a}, 2k\pi)$, the overlap is small (close to one). For examples, with the parameters for Fig. 1, when $\tau = 48\pi, 104\pi$ and 210π associated with the first minimum, the second maximum, and the third maximum, respectively, we have $|\langle \Psi(0) | \Psi(\tau) \rangle| = 0.103, 0.918$ and 0.994 . It is further

noted that the imaginary part of $\langle \Psi(0) | \Psi(210\pi) \rangle$ is very small. Thus, $\Psi(210\pi)$ is extremely close to the initial state. Therefore, from the time-dependent Schrödinger equation, we know that what happens during the interval $(0, 210\pi)$ will nearly exactly repeat again in the next interval $(210\pi, 420\pi)$, and so on. It implies the existence of another nearly periodic behavior. Thus, there are two distinct periodic behaviors. One has a period 2π , and the other one has a much longer period (say, for the above case, the period is 210π).

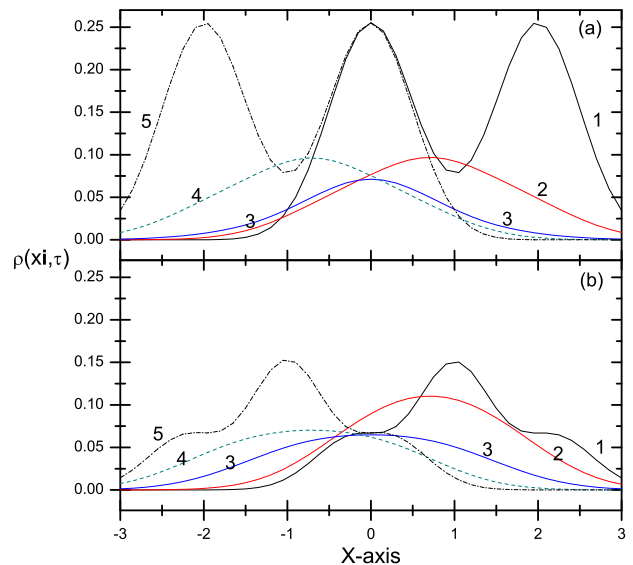


FIG. 3: (Color online) $\rho(\mathbf{r}_1, \tau)$ plotted along the X -axis. The curves "1" to "5" in 3a have τ from 0 to π with a step $\pi/4$. Those of 3b have τ from 48π to 49π with the same step. The parameters are the same as in Fig. 1.

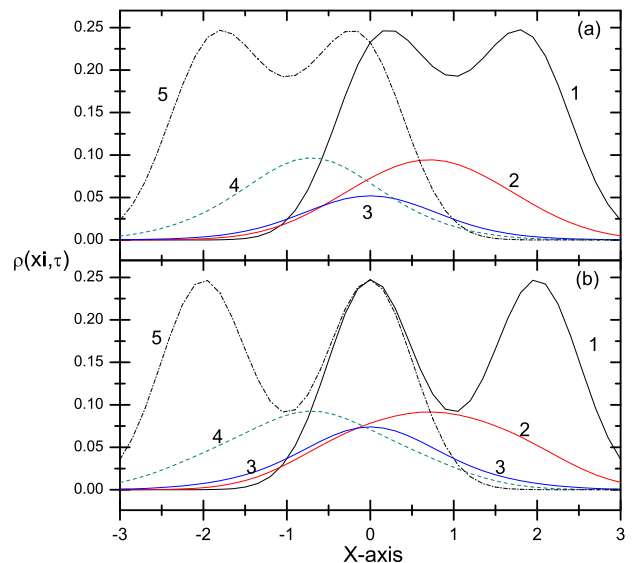


FIG. 4: (Color online) The same as Fig. 3, but the domain of τ is $(104\pi, 105\pi)$ in 4a and $(210\pi, 211\pi)$ in 4b.

The periodic behaviors can be shown in more detail by observing directly the densities. Let $\mathbf{r}_1 = x\mathbf{i}$, where \mathbf{i} is a unit vector along the X -axis. The distribution of $\rho(x\mathbf{i}, \tau)$ along the X -axis is plotted in Figs. 3 and 4, where τ is given at a number of values. Fig. 3a describes the evolution in the interval $(0, \pi)$, where the curve "1" is for the initial state. From "1" to "5" τ goes from 0 to π with a step $\pi/4$. One can see how the two particles undergo a round of collision. In fact, Fig. 1 and Fig. 3a describe the same thing except that ρ is plotted on the $X - Z$ plane in the former but only along the X -axis in the latter. When τ goes from π to 2π , the process occurring in $(0, \pi)$ will repeat again but in reverse direction. Thereby the cycle with the 2π period is completed. Fig. 3b describes the evolution in the interval $(48\pi, 49\pi)$ associated with the first minimum of the diamonds in Fig. 2. The peaks in 3b are much lower than those of 3a, and these peaks are located at different places. Therefore the system behaves differently in the two intervals, and the previous clear picture of a head-on collision becomes ambiguous. Fig. 4a is associated with the second maximum. The collision can be roughly seen but is not as clear as in Fig. 3a. Fig. 4b is associated with the third maximum, and is nearly identical to 3a. Therefore the cycle with the longer period is completed.

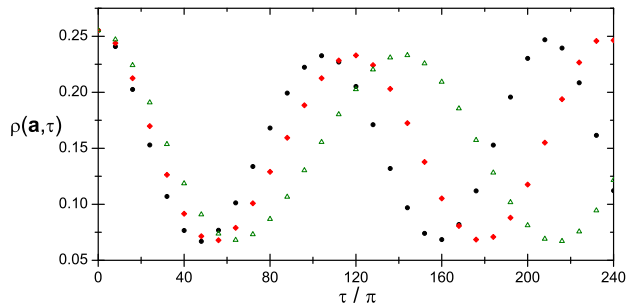


FIG. 5: (Color online) Similar to Fig. 2, but V_0 is fixed at 10 and c_6 has three choices: $-0.3r_0^6$, $-1.5r_0^6$ and $-3r_0^6$. The values of $\rho(\mathbf{a}, \tau)$ are, respectively, marked by black circles, red diamonds, and triangles. The other parameters are the same as in Fig. 1. This figure has a longer range than that in Fig. 2, and only the values of ρ with $\tau = 8k\pi$ are shown.

In Fig. 5, the strength of the attractive tail has been given at three values. In each case a slightly lower peak followed by a higher peak (the third maximum) appears again. With the three choices of c_6 , the third maximum appears at $\tau = 210\pi$, 236π , and 282π , respectively. At these three instants, $|\langle \Psi(0) | \Psi(\tau) \rangle|$ are all equal to 0.994 and the associated imaginary parts are very small. It implies a nearly exact recovery. Thus the nearly periodic behavior with the much longer period appears again. When $b \neq 0$ (i.e., the target particle is not at the center

initially), the above qualitative features remain. In particular, for a specific interaction, the longer period is not changed with b . Thus we conclude that the periodic phenomenon is common to trapping 2-body scatterings. It is emphasized that this phenomenon is sensitive to the interactions. A stronger repulsive (attractive) force would lead to a shorter (longer) long-period.

The accuracy of the above numerical results depends on K_{\max} . As an example selected values of $\rho(\mathbf{a}, \tau)$ are listed in Tab. I to show the dependence.

TABLE I: $\rho(\mathbf{a}, \tau)$ with three choices of K_{\max} . The parameters involved are the same as those for Fig. 1.

K_{\max}	12	16	20
$\rho(\mathbf{a}, 0)$	0.253	0.255	0.255
$\rho(\mathbf{a}, 50\pi)$	0.067	0.068	0.068
$\rho(\mathbf{a}, 100\pi)$	0.229	0.230	0.229

The convergency appears to be satisfying. Thus the numerical results obtained by using $K_{\max} = 20$ are accurate enough in qualitative sense.

In this paper the traditional 2-body scattering is considered under a new environment, namely, in a trap. Due to the trap, the two particles collide with each other repeatedly. Therefore, even the interaction is weak; the effect of interaction can be accumulated via the repeated collisions. Besides, comparing with the case of charged particles, the initial scattering states of neutral particles are more difficult to control. This disadvantage can be overcome by using optical traps. Furthermore, two periodic phenomena are found. They are essentially caused by the trap and by the interaction, respectively. The period of the latter is much longer and is sensitive to the interaction. Instead of measuring the differential cross section as usually does, the observation of the longer period and the details of the time-dependent density might be a valid source of information on weak interactions among neutral particles.

The above approach can be easily generalized to the cases with various interactions, and/or to the case of Fermion systems. It is reasonable to expect that the above trapped scattering could be experimentally realized via the progress of techniques in trapping neutral particles by optical traps.

Acknowledgments

The support from the NSFC under the grant 10874249 is appreciated.

[1] J. Stenger, S. Inouye, D. M. Stamper-Kurn, H.-J. Miesner, A. P. Chikkatur, and W. Ketterle, Nature (London) **396**,

- [2] M. D. Barrett, J. A. Sauer, and M. S. Chapman Phys. Rev. Lett. **87**, 010404 (2001).
- [3] P. Würtz, T. Langen, T. Gericke, A. Koglbauer, and H. Ott, Phys. Rev. Lett. **103**, 080404 (2009).
- [4] Z. B. Li, Z. F. Chen, Y. Z. He, and C. G. Bao, preprint, arXiv:0908.2929v1.
- [5] W. Tobocman, Nucl. Phys. A. **357**, 293 (1981).
- [6] M. Baranger, and K. T. R. Davies, Nucl. Phys. **79**, 403 (1966)
- [7] T. A. Brody and M. Moshinski, Monografias del Instituto de Fisica, Universidad Nacional Autonoma de Mexico (1960).